The external PL and EL quantum efficiencies of OC1C10-PPV blended with Bu-PBD have been quantitatively compared. The ratio of the EL and PL external efficiencies, $QE_{ext}(EL)/QE_{ext}(PL) \approx 0.5$, is well beyond the theoretical limit for strongly bound singlet and triplet excitons. A summary and discussion of the magnitude of the exciton binding energy in semiconducting polymers has recently been published; values range from less than 0.1 eV to as high as 1 eV (ref. 22). Efficient triplet-to-singlet conversion (for example, by triplet–triplet annihilation) before non-radiative recombination (with subnanosecond decay time) is unlikely in hydrocarbon polymers where the spin-orbit coupling is weak. Thus, the high value for QE(EL)/QE(PL) indicates either that the exciton binding energy is small or that the cross-section for an electron–hole pair to form a singlet bound state is significantly higher than the cross-section to form a triplet. Evidence of photogenerated triplet excitations has been reported (ref. 23 and references therein). However, the relevant timescale was in the millisecond regime or longer; hence, the observed triplets might be defect-stabilized.

Our results indicate that QE(EL)/QE(PL) can be large in polymer LEDs. The goal is to achieve balanced injection with high electron and hole currents in materials with large QE(EL). As high PL efficiencies (>60%) have been demonstrated[24], the achievement of efficient EL emission from polymer LEDs should be possible. □

Received 15 April; accepted 12 November 1998.

1. Burroughes, J. H. *et al.* Light-emitting diodes based on conjugated polymers. *Nature* **347,** 539–541 (1990).
2. Braun, D. & Heeger, A. J. Visible light emission from semiconducting polymer diodes. *Appl. Phys. Lett.* **58,** 1982–1984 (1991).
3. Bradley, D. D. C. Conjugated polymer electroluminescence. *Synth. Met.* **54,** 401–415 (1993).
4. Parker, I. D. Carrier tunneling and device characteristics in polymer light-emitting diodes. *J. Appl. Phys.* **75,** 1656–1666 (1994).
5. Campbell, I. H., Hagler, T. W., Smith, D. L. & Ferraris, J. P. Direct measurement of conjugated polymer electronic excitation energies using metal/polymer/metal structures. *Phys. Rev. Lett.* **76,** 1900–1903 (1996).
6. Richter, M. M., Fan, F., Klavetter, F., Heeger, A. J. & Bard, A. Electrochemistry and electrogenerated chemiluminescence of films of the conjugated polymer 4-methoxy-(2-ethylhexyloxy)-2,5-polyphenylenevinylene. *Chem. Phys. Lett.* **226,** 115–120 (1994).
7. Brom, P., Birgersson, J., Johansson, N., Logdland, M. & Salaneck, W. R. Calcium electrodes in polymer LEDs. *Synth. Met.* **74,** 179–181 (1995).
8. Yang, Y., Westerweele, E., Zhang, C., Smith, P. & Heeger, A. J. Enhanced performance of polymer light-emitting diodes using high-surface area polyaniline network electrodes. *J. Appl. Phys.* **77,** 694–698 (1995).
9. Gao, J., Heeger, A. J., Lee, J. Y. & Kim, C. Y. Soluble polypyrrole as the transparent anode in polymer light-emitting diodes. *Synth. Met.* **82,** 221–223 (1996).
10. Cao, Y., Yu, G., Zhang, C., Menon, R. & Heeger, A. J. Polymer light-emitting diodes with polyethylene dioxythiophene-polystyrene sulfonate as the transparent anode. *Synth. Met.* **87,** 171–174 (1997).
11. Kuhn, H. Classical aspects of energy transfer in molecular systems. *J. Chem. Phys.* **53,** 101–108 (1970).
12. Greenham, N. C. Understanding the limits to performance in electronic devices based on PPV. *Bull. Am. Phys. Soc.* **43 (1),** 14 (1998).
13. Blom, P. W. M., de Jong, M. J. M. & Vleggaar, J. J. M. Electron and hole transport in poly(p-phenylene vinylene). *Appl. Phys. Lett.* **68,** 3308–3310 (1996).
14. Blom, P. W. M., de Jong, M. J. M. & Munster, M. G. Electric-field and temperature dependence of the hole mobility in poly(p-phenylene vinylene). *Phys. Rev. B* **55,** 656–659 (1997).
15. Blom, P. W. M., de Jong, M. J. M. & Breedijk, S. Temperature dependence electron-hole recombination in polymer light-emitting diodes. *Appl. Phys. Lett.* **71,** 930–932 (1997).
16. Greenham, N. C. *et al.* Measurement of absolute photoluminescence quantum efficiencies in conjugated polymer. *Chem. Phys. Lett.* **241,** 89–96 (1995).
17. Schmidt, A., Anderson, M. L. & Armstrong, N. R. Electronic states of vapor deposited electron and hole transport agents and luminescent materials for light-emitting diodes. *J. Appl. Phys.* **78,** 5619–5625 (1995).
18. Kersting, R. *et al.* Ultrafast field-induced dissociation of excitons in conjugated polymers. *Phys. Rev. Lett.* **73,** 1440–1443 (1994).
19. Moses, D. *et al.* Mechanism of carrier generation in poly(phenylene vinylene): Transient photoconductivity and photoluminescence at high fields. *Phys. Rev. B* **54,** 4748–4754 (1996).
20. Greenham, N. C., Friend, R. H. & Bradley, D. D. C. Angular dependence of the emission from a conjugated polymer light-emitting diode: implications for efficiency calculations. *Adv. Mater.* **6,** 491–494 (1994).
21. Lemmer, U. *et al.* Electroluminescence from poly(phenylene vinylene) in a planar metal-polymer-metal structure. *Appl. Phys. Lett.* **68,** 3007–3009 (1996).
22. Sariciftci, N. S. (ed.) *Primary Photoexcitations in Conjugated Polymers: Molecular Excitons vs Semiconductor Band Model* (World Scientific, Singapore, 1997).
23. Smilowitz, L. & Heeger, A. J. Photoinduced absorption from triplet excitations in poly(2-methoxy,5-(2′-ethylhexyloxy)-p-phenylene vinylene) oriented by gel processing in polyethylene. *Synth. Met.* **48,** 193–196 (1992).
24. Hide, F. *et al.* Semiconducting polymers: a new class of solid state laser materials. *Science* **273,** 1833–1836 (1996).

Acknowledgements. Research at UNIAX was partially supported by the Office of Naval Research.

Correspondence and requests for materials should be addressed to A.J.H.

Hybrid hydrogels assembled from synthetic polymers and coiled-coil protein domains

Chun Wang*, Russell J. Stewart* & Jindřich Kopeček*†

*Departments of * Bioengineering and † Pharmaceutics and Pharmaceutical Chemistry, University of Utah, Salt Lake City, Utah 84112, USA*

Stimuli-sensitive polymer hydrogels, which swell or shrink in response to changes in the environmental conditions, have been extensively investigated and used as 'smart' biomaterials and drug-delivery systems[1,2]. Most of these responsive hydrogels are prepared from a limited number of synthetic polymers and their derivatives, such as copolymers of (meth)acrylic acid, acrylamide and *N*-isopropyl acrylamide[3–12]. Water-soluble synthetic polymers have also been crosslinked with molecules of biological origin, such as oligopeptides[13] and oligodeoxyribonucleotides[14], or with intact native proteins[15]. Very often there are several factors influencing the relationship between structure and properties in these systems, making it difficult to engineer hydrogels with specified responses to particular stimuli. Here we report a hybrid hydrogel system assembled from water-soluble synthetic polymers and a well-defined protein-folding motif, the coiled coil. These hydrogels undergo temperature-induced collapse owing to the cooperative conformational transition of the coiled-coil protein domain. This system shows that well-characterized water-soluble synthetic polymers can be combined with well-defined folding motifs of proteins in hydrogels with engineered volume-change properties[16,17].

The coiled coil[18], a left-handed superhelix of two or more right-handed α-helices, has been identified in proteins ranging from

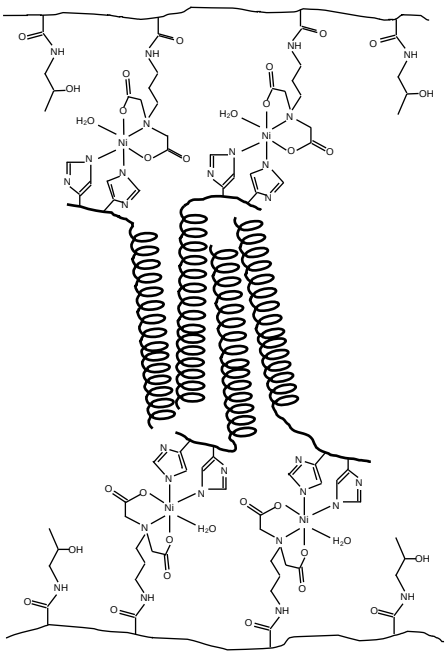

Figure 1 Structural representation of the hybrid hydrogel primary chains and the attachment of His-tagged coiled-coil proteins. Poly(HPMA-co-DAMA) is shown here as the primary chains. The pendant iminodiacetate groups form complexes with transition-metal ions, such as Ni^{2+}, to which the terminal histidine residues of the coiled coils are attached. A tetrameric coiled coil (not drawn to scale), consisting of two parallel dimers associating in an antiparallel fashion, is shown here as an example of many of the possible conformations.

muscle proteins to DNA transcription factors. It has the characteristic amino-acid heptad repeating units designated as 'a' to 'g' with hydrophobic residues at positions 'a' and 'd', and polar residues at other positions. Many native and *de novo* designed coiled coils can undergo conformational transition in response to temperature, pH, ionic strength, solvent and so forth. Dramatic changes in coiled-coil stability, conformation, and responsiveness towards the external environment can be caused by minor alteration of the primary structure; such alterations can occur through natural evolution[19], experimental mutagenesis[20] or *de novo* design[21,22]. We hypothesized that by using coiled coils with engineered sequences as crosslinks for synthetic polymer chains, we would be able to prepare hybrid hydrogels (Fig. 1) with predetermined stimuli sensitivity reflecting the structure and properties of coiled coils.

For the primary chains of our hybrid hydrogels (Fig. 1), we prepared a linear hydrophilic copolymer of *N*-(2-hydroxypropyl)-methacrylamide (HPMA)[13], and a metal-chelating monomer *N*-(*N*′,*N*′-dicarboxymethylaminopropyl)methacrylamide (DAMA), by radical copolymerization. A metal complex is formed (Fig. 1) by the pendant metal-chelating ligand—iminodiacetate (IDA)-Ni^{2+} and the terminal histidine residues (His tag) of the coiled coils. Similar schemes have been used for purifying recombinant proteins[23] and immobilizing them on interfaces[24,25]. Here it serves as a simple, convenient way of anchoring genetically engineered His-tagged coiled coils to the hydrogel primary chains.

Two His-tagged coiled coils were used to assemble hybrid hydrogels. The first, designated CC1, was a natural protein sequence corresponding to a segment of the stalk region (amino acid, a.a., 336 to 590, Fig. 2a) of the motor protein kinesin[26]. Although native kinesin is homodimeric, sedimentation equilibria experiments indicated that CC1 was predominantly tetrameric (data not shown). The circular dichroism (CD) spectrum of CC1 has the characteristic feature of an α-helical coiled coil (Fig. 2b). CC1 showed a major cooperative conformational change at 35 °C and a minor one at 65 °C (Fig. 2c). Stability experiments with the separate coiled-coil regions (our unpublished data) demonstrated that these two transitions were respectively due to the unfolding of the longer and the shorter coiled-coil regions of CC1 (Fig. 2a). The CD signal

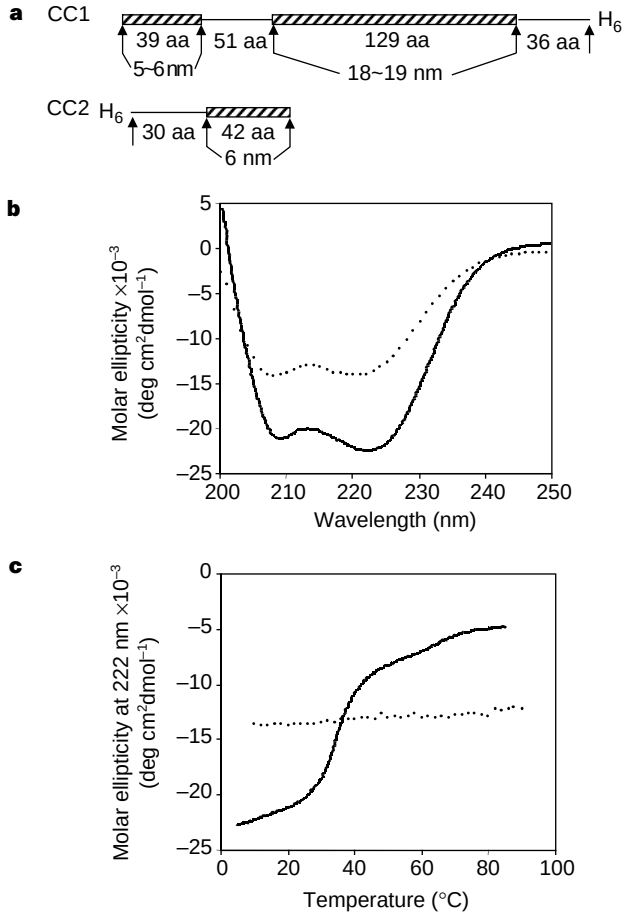

Figure 2 The coiled coils and characterization by circular dichroism. **a**, The block diagrams of the two proteins (CC1 and CC2). The amino-acid (aa) sequence of the EK42 domain is $(VSSLESK)_6$. The region separating the EK42 domain and the His tag is GMASMTGGQQMGRDLYDDDDKDP. The numbers of amino-acid residues in the coiled-coil and non-coiled-coil domains are given. The length of the coiled-coil domains was estimated according to ref. 28. **b**, CD spectra of the two proteins (solid line, CC1; dotted line, CC2) in PBS at 25 °C. The ratios of molar ellipticity minima at 222 and 208 nm were close to 1.0, typically found for α-helical coiled coils[27]. **c**, Thermal unfolding of both proteins (solid line: CC1; dotted line: CC2) in PBS as monitored by the change in molar ellipticity at 222 nm wavelength.

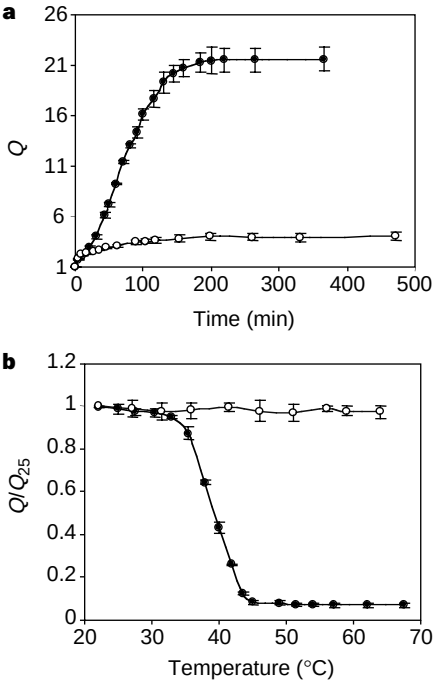

Figure 3 Dynamic swelling and the temperature-induced volume transition of the hybrid hydrogels in PBS. The extent of gel swelling was determined by measuring the two-dimensional changes of gel pieces of various shapes. For example, the changes of the three sides of a triangular gel piece were measured based on the optical images taken at different times during the course of gel swelling. The dimensional changes along different directions were found to be the same, within experimental error, indicating three-dimensional isotropic swelling of the hydrogel networks. Filled circles, gel 1; open circles: gel 2. **a**, Dynamic swelling characterized as the volume swelling ratio Q versus time. The one-dimensional swelling ratio is defined as L/L_0, where L is the size of the swollen gel, and L_0 is the corresponding size of the dried gel. L and L_0 were determined from optical images of the gels. These images were obtained using a Nikon Eclipse E800 optical microscope, and photographs were taken with a CCD camera. Assuming three-dimensional isotropic swelling, the volume swelling ratio Q was calculated as $(L/L_0)^3$. **b**, Effect of temperature on the gel swelling behaviour. Q/Q_{25} is the ratio of the equilibrium volume swelling ratio of gels at an elevated temperature and the equilibrium volume swelling ratio at 25 °C in the same buffer. Gels were placed in a cuvette with a jacket connected to a water bath. The rate of temperature increase was 1 °C min^{-1}, with equilibration time of 2 min. The temperature of the water bath was calibrated by measuring the temperature inside the cuvette with a thermocouple. The error bars represent the standard deviation of three separate measurements.

of folded CC1 was fully restored after a temperature cycle, indicating a reversible folding–unfolding process.

The second protein, CC2, contains a *de novo* designed coiled-coil sequence (EK42) and a terminal His tag separated by a non-coiled-coil region of 30 amino acids (Fig. 2a). EK42 was previously designed to form parallel dimeric coiled coils[27], based on the principles that are thought to govern the folding and oligomerization of many native coiled coils and synthetic model peptides. Sedimentation equilibria measurements, however, revealed that CC2 forms tetramers in solution (data not shown). The CD spectrum of CC2 suggested an α-helical coiled-coil conformation (Fig. 2b). Compared with previous data on EK42[27], the thermal stability of CC2 was unexpectedly high, as shown by melting experiments (Fig. 2c). CC2 did melt, in a cooperative fashion similar to that observed for CC1, at temperatures under 90 °C in the presence of a denaturing agent, guanidine hydrochloride (GuHCl). The melting temperature (T_m) of CC2 was linearly related to the GuHCl concentration (data not shown). Thus we estimated the T_m of CC2 in the absence of GuHCl to be ~108 °C by extrapolation to zero GuHCl concentration. The unexpectedly high stability of CC2 may be due to the presence of the non-coiled-coil spacer sequence (Fig. 2a).

Hybrid hydrogels were assembled by mixing the chelating copolymer of HPMA charged with Ni^{2+} and the coiled-coil proteins, CC1 and CC2. Homogeneous films were obtained after drying the mixed solutions on Teflon sheets. Using the same procedure, control films were prepared with: (1) chelating copolymer and Ni^{2+} without coiled coils, (2) coiled coils without the chelating copolymer or Ni^{2+}, and (3) chelating copolymer and coiled coil without Ni^{2+}.

To verify the formation of hydrogels, the dried films were rehydrated in phosphate buffer (20 mM sodium phosphate, pH 7.4) in the absence of salt. The control films dissolved readily on immersion in the buffer. In contrast, the films formed with all the components—chelating HPMA copolymer, Ni^{2+} and the coiled coils—remained physically intact for 2 h before disintegrating due to excess swelling. Moreover, in the presence of 150 mM NaCl, these films remained physically intact for at least 24 h. Adding imidazole, which competes with the His tags for Ni^{2+}, increased the swelling of the gels at moderate concentrations (for example, 100 mM) and dissolved the gels at higher concentrations (such as 500 mM). These observations indicated that three-dimensional hybrid hydrogels were created as a result of the specific interactions proposed in Fig. 1. Gels assembled with CC1 and CC2 were designated as gel 1 and gel 2, respectively. Swelling profiles of these gels were studied in phosphate buffered saline (PBS; 20 mM sodium phosphate, 150 mM NaCl, pH 7.4) (Fig. 3a). The swelling was fast at first, more than doubling the dried gel volume in less than 10 min after being submerged in PBS. After about 3 h, swelling of the gels approached equilibrium. During the next 24 h, the gel volume increased slightly owing to the relaxation of the polymeric chains, as the force of hydration balanced the elastic constraint of the three-dimensional gel network. The same copolymer precursor was used in gel preparation and both coiled coils were similarly charged. The difference in swelling kinetics and equilibrium swelling ratio may be due to the considerable difference in the size of the proteins (Fig. 2a), the difference in gel crosslinking density, and/or the difference in the polymer–solvent interaction parameter, χ.

We investigated the temperature-responsiveness of the hybrid hydrogels containing CC1 and CC2, which exhibited different thermal stability in solution. On an increase in temperature from 25 °C to 70 °C, gel 1 underwent a sudden collapse to 10% of its equilibrium volume at 25 °C, with a mid-point transition temperature of 39 °C (Fig. 3b). This mid-point temperature of gel collapse was in good agreement (within 5 °C) with the T_m of the main coiled-coil region of CC1 as determined by CD. In contrast, no change in swelling was observed for gel 2 over 25 °C to 70 °C, as expected from the CD melting data for CC2 in solution.

We propose that the gel structural transition is caused by the temperature-induced conformational change in the CC1 coiled coil. CC1 is largely a rigid elongated 'rod' with extended coiled-coil structure; around 170 of the 255 amino acid residues of CC1 have strong propensity for adopting the coiled-coil conformation (Fig. 2a). The length of the CC1 bundle was estimated from the electron micrographs[28] to be about 25–30 nm. As the protein unfolds, there would be a considerable decrease in the hydrodynamic radius of the individual molecules from the initial elongated rods to random coils that caused the gels to collapse. Although such a conformational transition of CC1 was reversible in solution, the temperature-induced gel transition was not reversible within the relatively short period of time of the experiments (48 h). Physical constraints from the synthetic copolymer backbones and chain entanglement through exposed hydrophobic patches of the coiled coils could be contributing factors.

Our hybrid hydrogel system possesses several distinct features. The use of metal complexation as a means of anchoring His-tagged proteins should be applicable to all recombinant proteins with this affinity tag. Other metal ions, such as Zn^{2+} and Ga^{2+}, could be used instead of Ni^{2+}, for purposes such as stabilizing proteins, or tracking the hydrogels *in vivo* using magnetic resonance imaging (MRI). Unlike responsive gels formed solely by self-assembly of protein molecules containing α-helices[29] and β-sheets[30], this hybrid hydrogel system preserves the benefit of using synthetic polymer backbones that are well characterized, easy to manufacture and biocompatible. Furthermore, it offers the possibility of creating hydrogels of unusual physicochemical and/or biological properties by tailoring the coiled coils using techniques of molecular biology. For example, coiled coils with different T_m values could be used to assemble hybrid hydrogels that would display accordingly different gel structural transition temperatures. Moreover, two or more of these coiled coils could be used simultaneously, resulting in gels capable of stepwise transitions with each step triggered at a different temperature, which is difficult to achieve using hydrogels of synthetic polymers alone. The hybrid hydrogel system we describe here may also be useful for incorporating and delivering therapeutic proteins. Because these hydrogels are assembled in aqueous solvents, the biological activities of the protein drugs could be preserved. □

Methods

Construction of CC1 expression vector. A segment of DNA encoding the region of the *Drosophila* kinesin stalk from amino acid Val 336 to amino acid Ser 590 was PCR-amplified. To facilitate subcloning of the PCR product, the coding primer (5′-GGTCTAGAGTGGTCTGCGTTAACGAG-3′) containing a terminal *Xba*I site and the non-coding primer (5′-CCCCGGCGAGTCCA GCCTCGAGCC-3′) containing a terminal *Ava*I site were used. Following digestion with *Xba*I and *Ava*I, the PCR product was ligated into the pET21a expression vector (Novagen, Madison, WI), which had been digested with *Nhe*I and *Ava*I. The CC1 vector expressed kinesin stalk protein which had, at the amino terminus, the additional sequence Met-Ala-Arg, and at the carboxy terminus the appended sequence Leu-Glu-His-His-His-His-His-His. The correct construct was verified by direct sequencing.

Construction of CC2 expression vector. An artificial gene encoding the EK42 domain was constructed from six synthesized single-stranded oligonucleotides by mixing the complementary strands to form three duplexes, which were ligated into the expression vector pRSETB (Invitrogen, Carlsbad, CA), cut with *Bam*HI and *Eco*RI, and modified to contain a kanamycin-resistance gene. The correct construct was verified by direct sequencing.

Protein expression and purification. Both proteins were expressed in *Escherichia coli* BL21(DE3)pLysS (Novagen, Madison, WI) using isopropyl β-thiogalactoside (IPTG) as the inducing agent, and were purified from soluble portion of cell lysate using Ni-NTA metal affinity resin (Qiagen, Santa Clarita, CA). SDS-polyacrylamide gel electrophoresis, amino-acid analysis and matrix-assisted laser desorption ionization time-of-flight mass spectrometry (MALDI-TOF MS) were used to verify the identity and purity of the proteins.

Circular dichroism. The measurements were performed at 25 °C in PBS using an Aviv 62DS CD spectrometer equipped with a thermoelectric temperature control system and a 1.0-cm-pathlength quartz cuvette. Protein concentration used was 4 μM. Wavelength scans (1-nm bandwidth, 1 nm per step, and 5-s data averaging) for each sample were repeated five times, averaged, corrected by subtracting the buffer spectrum, and smoothed. For thermal melting experiments, the CD signal at 222 nm was monitored as temperature was increased from 10 to 90 °C with 0.1 or 2 °C per step. At each temperature, the sample was equilibrated for 5 min followed by 60 s of data point averaging. The transition temperatures were determined from the first-order differentiation of the melting curves.

Chemical syntheses. *N*-(*N*′,*N*′-dicarboxymethylaminopropyl)methacrylamide (DAMA) was synthesized by reacting bromoacetic acid (14 mmol, 2.0 g) with *N*-(3-aminopropyl)methacrylamide hydrochloride (7 mmol, 1.25 g) at alkaline pH. The reaction was allowed to progress for 2 h at 0 °C, then for 48 h at room temperature. DAMA was recrystallized from anhydrous ethanol; yield, 0.5 g (30%); melting point, 178–180 °C. DAMA was characterized by thin layer chromatography, mass spectrometry, proton nuclear magnetic resonance and elemental analysis. Copolymerization of DAMA and HPMA was performed in methanol (86.9 wt%) with 2,2′-azobisisobutyronitrile (AIBN, 0.6 wt%) as initiator. The reaction progressed in nitrogen atmosphere at 50 °C for 24 h. The copolymer was precipitated into acetone, dialysed against water, and lyophilized. Relative molecular mass (240,000) and polydispersity (1.68) were measured by size exclusion chromatography on a fast protein liquid chromatography system equipped with a Superose 6 (10/30) column (Pharmacia, Piscataway, NJ) and a light-scattering detector (MiniDawn, Wyatt). The column was calibrated using polyHPMA fractions with small polydispersity. The content of carboxylic groups (15 mol%) was determined by acid–base titration using a 10-ml ABU80 autoburette and a PHM84 research pH meter.

Hybrid hydrogel preparation. To prepare the metal-charged copolymer precursor, a solution of poly(HPMA-co-DAMA) (200 mg dissolved in 10 ml of deionized water with pH adjusted by 1 M NaOH to 7.5–7.8) was mixed with excess Ni^{2+} (10 ml of 0.1 M $NiSO_4$ with pH adjusted by NaOH to 7.1) under constant stirring, in order to prevent premature crosslinking of the copolymer precursors. The copolymer–Ni^{2+} complex was separated from the excess free Ni^{2+} using a size exclusion column packed with Sephadex G-25 beads (Pharmacia, Piscataway, NJ) equilibrated with deionized water. To prepare the hybrid hydrogels, the coiled-coil proteins (2 mg of each dissolved in 0.1 ml of deionized water) were separately added to, and mixed with, solutions of the copolymer–Ni^{2+} complex (0.55 mg in 0.1 ml of deionized water for gel 1, and 1.1 mg in 0.2 ml of deionized water for gel 2). The mixed solutions were dropped on a Teflon sheet with 50 μl per drop, and dried at room temperature and atmospheric pressure. Thin films of gels formed were circular, with diameter of 5 mm and thickness of ~0.1 mm. They were cut and stored in a desiccator at 25 °C for use in swelling studies.

Received 14 September; accepted 27 November 1998.

1. Langer, R. Drug delivery and targeting. *Nature* **392** (suppl.), 5–10 (1998).
2. Peppas, N. A. Hydrogels and drug delivery. *Curr. Opin. Colloid Interface Sci.* **2,** 531–537 (1997).
3. Kopeček, J., Vacík, J. & Lím, D. Permeability of membranes containing ionogenic group. *J. Polym. Sci.* A-**1, 9,** 2801–2815 (1971).
4. Suzuki, A. & Tanaka, T. Phase transition in polymer gels induced by visible light. *Nature* **346,** 345–347 (1990).
5. Kokufuta, E., Zhang, Y. Q. & Tanaka, T. Saccharide-sensitive phase transition of a lectin-loaded gel. *Nature* **351,** 302–304 (1991).
6. Kwon, I. C., Bae, Y. H. & Kim, S. W. Electrically erodible polymer gel for controlled release of drugs. *Nature* **354,** 291–293 (1991).
7. Osada, Y., Okuzaki, H. & Hori, H. A polymer gel with electrically driven motility. *Nature* **355,** 242–244 (1992).
8. Chen, G. & Hoffman, A. S. Graft copolymers that exhibit temperature-induced phase transitions over a wide range of pH. *Nature* **373,** 49–52 (1995).
9. Yoshida, R. *et al.* Comb-type grafted hydrogels with rapid de-swelling response to temperature changes. *Nature* **374,** 240–242 (1995).
10. Holtz, J. H. & Asher, S. A. Polymerized colloidal crystal hydrogel films as intelligent chemical sensing materials. *Nature* **389,** 829–832 (1997).
11. Hu, Z., Chen, Y., Wang, C., Zheng, Y. & Li, Y. Polymer gels with engineered environmentally responsive surface patterns. *Nature* **393,** 149–152 (1998).
12. Kiser, P. F., Wilson, G. & Needham, D. A synthetic mimic of the secretory granule for drug delivery. *Nature* **394,** 459–462 (1998).
13. Šubr, V., Duncan, R. & Kopeček, J. Release of macromolecules and daunomycin from hydrophilic gels containing enzymatically degradable bonds. *J. Biomater. Sci. Polym. Edn* **1,** 261–278 (1990).
14. Nagahara, S. & Matsuda, T. Hydrogel formation via hybridization of oligonucleotides derivatized in water-soluble vinyl polymers. *Polym. Gels Networks* **4,** 111–127 (1996).
15. Obaidat, A. A. & Park, K. Characterization of glucose dependent gel-sol phase transition of the polymeric glucose-concanavalin A hydrogel system. *Pharm. Res.* **13,** 989–995 (1996).
16. Wang, C., Stewart, R. J. & Kopeček, J. De novo design of hybrid hydrogels: water soluble polymers crosslinked by coiled-coil protein domains. *Proc. Int. Symp. Controlled Release Bioact. Mater.* **25,** 54–55 (1998).
17. Wang, C., Stewart, R. J. & Kopeček, J. Tailor-made hybrid hydrogels: synthetic macromolecules crosslinked by coiled-coil protein domains. *ACS Polym. Preprints* **39,** 194–195 (1998).
18. Lupas, A. Coiled coils: new structures and new functions. *Trends Biochem. Sci.* **21,** 375–382 (1996).
19. O'Shea, E. K., Rutkowski, R. & Kim, P. S. Mechanism of specificity in the Fos-Jun oncoprotein heterodimer. *Cell* **68,** 699–708 (1992).
20. Harbury, P. B., Zhang, T., Kim, P. S. & Alber, T. A switch between two-, three-, and four-stranded coiled coils in GCN4 leucine zipper mutants. *Science* **262,** 1401–1407 (1993).
21. Su, J. Y., Hodges, R. S. & Kay, C. M. Effect of chain length on the formation and stability of synthetic α-helical coiled coils. *Biochemistry* **33,** 15501–15510 (1994).
22. Gonzalez, L. Jr, Plecs, J. J. & Alber, T. An engineered allosteric switch in leucine-zipper oligomerization. *Nature Struct. Biol.* **3,** 510–515 (1996).
23. Hochuli, H. Purification of recombinant proteins with metal chelate adsorbent. *Genet. Eng.* **12,** 87–98 (1990).
24. Ng, K., Pack, D. W., Sasaki, D. Y. & Arnold, F. H. Engineered protein-lipid interactions: targeting of histidine-tagged proteins to metal-chelating lipid monolayers. *Langmuir* **11,** 4048–4055 (1995).
25. Ho, C. H., Limberis, L., Caldwell, K. D. & Stewart, R. J. A metal-chelating pluronic for immobilization of histidine-tagged proteins at interfaces: immobilization of firefly luciferase on polystyrene beads. *Langmuir* **14,** 3889–3894 (1998).
26. Yang, J. T., Laymon, R. A. & Goldstein, L. S. B. A three-domain structure of kinesin heavy chain revelaed by DNA sequence and microtubule binding analyses. *Cell* **56,** 879–889 (1989).
27. Graddis, T. J., Myszka, D. G. & Chaiken, I. M. Controlled formation of model homo- and heterodimer coiled coil polypeptides. *Biochemistry* **32,** 12664–12671 (1993).
28. Hirokawa, N. *et al.* Submolecular domains of bovine brain kinesin identified by electron microscopy and monoclonal antibody decoration. *Cell* **56,** 867–878 (1989).
29. Petka, W. A., Harden, J. L., McGrath, K. P., Wirtz, D. & Tirrell, D. A. Reversible hydrogels from self-assembling artificial proteins. *Science* **281,** 389–392 (1998).
30. Aggeli, A. *et al.* Responsive gels formed by the spontaneous self-assembly of peptides into polymeric β-sheet tapes. *Nature* **386,** 259–262 (1997).

Acknowledgements. This work was supported in part by the Center for Biopolymers at Interfaces (CBI) and the University of Utah Research Foundation.

Correspondence and requests for materials should be addressed to J.K. (e-mail: Jindrich.Kopecek@m.cc.utah.edu).

A complex clathrate hydrate structure showing bimodal guest hydration

Konstantin A. Udachin & John A. Ripmeester

Steacie Institute for Molecular Sciences, National Research Council of Canada, Ottawa, Ontario, Canada K1A 0R6

Interactions between hydrophobic groups in water[1], as well as biomolecular hydration more generally[2–4], are intimately connected to the structure of liquid water around hydrophobic solutes. Such considerations have focused interest on clathrate hydrates: crystals in which a hydrogen-bonded network of water molecules encages hydrophobic guest molecules with which the water interacts only by non-directional van der Waals forces. Three structural families of clathrate hydrates have hitherto been recognized: cubic structure I ($2M_S{\cdot}6M_L{\cdot}46H_2O$) (ref. 5), cubic structure II ($16M_S{\cdot}8M_L{\cdot}136H_2O$) (ref. 5) and hexagonal structure H ($M_L{\cdot}3M_S{\cdot}2M_S{\cdot}34H_2O$) (refs 6, 7) hydrates (here M_L and M_S are the hydrophobic guest sites associated with large and small cavities, respectively). Here we report a new hydrate structure: 1.67 choline hydroxide·tetra-*n*-propylammonium fluoride·30.33H_2O. This structure has a number of unusual features; in particular the choline guest exhibits both hydrophobic and hydrophilic modes of hydration. Formally the structure consists of alternating stacks of structure H and structure II hydrates, and might conceivably be found in those settings (such as seafloor deposits over natural-gas fields) in which clathrate hydrates form naturally.

The classical clathrate structures are three-dimensional lattices that can be built up by fitting together different types of closed cages composed of 4-, 5- and 6-sided polygons (Table 1). Both in experimental work and modelling studies on biomolecular hydration, structural features such as closed pentagonal rings of hydrogen-bonded water molecules are taken as evidence for clathrate-like hydrophobic hydration[2–4]. Although this notion generally